

**J. JANÁK, S. SLOVÍK, Z. FAŠKOVÁ,
K. MIKULA**

DISTURBING POTENTIAL AND ITS GEOMETRICAL PROPERTIES

Juraj JANÁK

email: juraj.janak@stuba.sk
Department of Theoretical Geodesy

Stanislav SLOVÍK

email: alifunes@gmail.com
Department of Theoretical Geodesy

Zuzana FAŠKOVÁ

email: zuzana.faskova@stuba.sk
Department of Mathematics and Descriptive Geometry

Karol MIKULA

email: karol.mikula@stuba.sk
Department of Mathematics and Descriptive Geometry

Research field: physical geodesy, gravimetry, finite element method, PDEs.

Address:

Faculty of Civil Engineering
Slovak University of Technology, Radlinského 11
813 68 Bratislava, Slovakia
Tel: +421 (2) 5927 4537

ABSTRACT

Disturbing potential is probably the most crucial quantity in gravity field modelling. Usually, the disturbing potential is converted into a geoid height or height anomaly and presented as a contour map of a geoid or quasigeoid. In our contribution we present a spatial geometry of the equipotential surfaces of the disturbing potential around the Earth. The models presented are solutions of a mixed boundary value problem; they combine the Neumann and Dirichlet boundary conditions, and are solved using the Finite Element Method. The boundary values are generated from an EGM2008 geopotential model. However, the combination of the terrestrial measurement and the satellite gravity gradiometry-originated data can be used in the future. Therefore this work can be seen as a preliminary study before the exploitation of the actual gravity gradiometry data. The disturbing potential model is presented in the form of a 3D model up to an altitude of 20000km above the Earth's surface.

1 INTRODUCTION

Let us start with an obvious representation of the geometry of the Earth's actual gravity field. Usually we visualize a geoid and other (mostly external) equipotential surfaces of gravity potential. However, in practical computations we work more frequently with a disturbing gravity field. Let us think about how the equipotential surfaces of disturbing potential look like and what are their basic properties. The idea of visualizing a disturbing gravity field started from pure curiosity, but later some advantages compared to the classical representation of a gravity field and some possible applications appeared. In order to be able to plot the equipotential surfaces of disturbing

potential around the Earth, some efficient computational method, which would be able to fill a certain selected volume with the values of a disturbing potential, needs to be found. We determined that the Finite Element Method (FEM), see e.g. (Brenner and Scott, 2002), which is well known in several engineering applications, is one of the most appropriate methods. This method has already been successfully used to solve geodetic boundary value problems (Fašková et al., 2010). An advantage of the formulation of the boundary value problem with the consequent application of the FEM against the simple utilization of a spherical harmonic synthesis is that it can adopt different types of data and also combine satellite and terrestrial data in one very detailed solution.

KEY WORDS

- *Disturbing potential,*
- *Finite Element Method,*
- *Ansys*

2 MATHEMATICAL AND PHYSICAL BACKGROUND

Let us start with the definition of the disturbing potential T :

Definition 1: A disturbing potential T is a scalar quantity which is obtained as the difference between the gravity potential W and the normal gravity potential U at the same point in the following sense, see e.g. *Vaniček and Krakiwsky (1986)*

$$T = W - U. \quad (1)$$

As both functions W and U contain the same centrifugal potential, it is also possible to obtain a disturbing potential T as the difference between the gravitation potential V and the normal gravitation potential U_g . Thus, the disturbing potential inherits some basic properties of a gravitation potential; it is also harmonic in a space without masses. Applying the gradient operator to the disturbing potential, we get

$$\nabla T = \nabla(W - U) = \nabla W - \nabla U. \quad (2)$$

Taking into account the relations $\nabla W = \vec{g}$ and $\nabla U = \vec{\gamma}$, we get

$$\nabla T = \vec{g} - \vec{\gamma} = \vec{\delta g}, \quad (3)$$

where $\vec{\delta g}$ is known as a gravity disturbance vector (*Hofmann-Wellenhof and Moritz, 2005*), see Fig. 1.

The angle θ in Fig. 1 is called a deflection of the vertical. Based on Eq. (3) the gravity disturbance vector is perpendicular to the equipotential surface of the disturbing potential. We should be

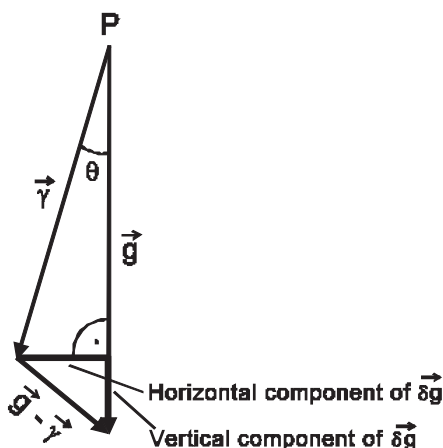


Fig. 1 Geometry of a gravity disturbance vector

aware that the gravity disturbance vector can reach an arbitrary direction, even a horizontal direction, as the horizontal component of $\vec{\delta g}$ can be significant (about 140 mGal for $\theta = 30''$).

The general equation of an equipotential surface of a gravity potential reads

$$W(\vec{r}) = \text{const.} \quad (4)$$

Let us recall some basic properties of these surfaces: they are closed, smooth, continuous, convex everywhere, never cross each other and convergent towards the poles. Analogously with eq. (4), we can write the general equation of an equipotential surface of a disturbing potential as

$$T(\vec{r}) = \text{const.} \quad (5)$$

It is interesting to investigate what the properties of the equipotential surfaces of a disturbing potential are. We will look for these properties throughout our paper and summarize them in the conclusion.

In Fig. 2, we can see the disturbing potential at the Earth's surface computed from the Earth Geopotential Model EGM08 (*Pavlis et al., 2008*).

The isolines in the map, which are given by gray scale border lines, represent the intersections of particular surfaces $T(\vec{r}) = \text{const.}$ with the Earth's surface. The most important isoline is $T = 0$, which divides the Earth's surface into two parts, where the disturbing potential is respectively positive and negative.

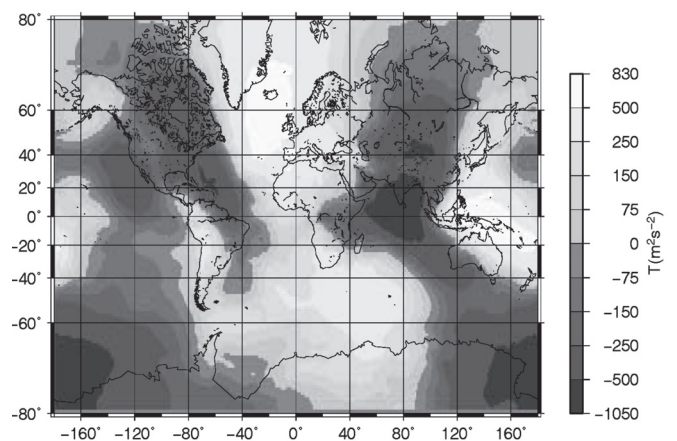


Fig. 2 Disturbing potential at the Earth's surface computed from the EGM08, units: $\text{m}^2 \cdot \text{s}^{-2}$

3 NUMERICAL EXPERIMENT USING THE FINITE ELEMENT METHOD

In order to investigate the features of the equipotential surfaces of disturbing potential $T(\vec{r}) = \text{const.}$, we first formulated the boundary value problem for the disturbing potential in almost the entire global domain around the Earth up to selected altitude (except for the small conical parts above the North and South Poles); we then implemented the Finite Element Method (FEM) to solve this problem. The FEM solution was performed using ANSYS software (<http://www.ansys.com>). We got a spatial grid of nodes with the known value of disturbing potential T as the numerical result. Consequently, we used the 3D visualization Voxler[®] software from Golden Software to visualize our results.

The computational domain Ω for the boundary value problem was constructed assuming a spherical approximation of the earth, as can be seen in Figs. 3 and 4. The Eastern and Western hemispheres were computed separately. Fig. 3 shows the meridian section across one computational domain, while Fig. 4 contains its 3D image.

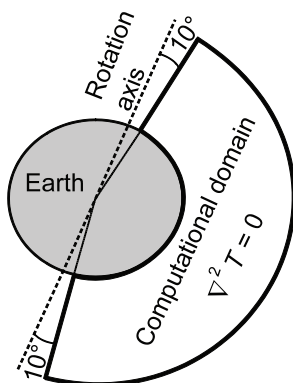


Fig. 3 Meridian section across the computational domain. The boundary is represented by the thick solid line

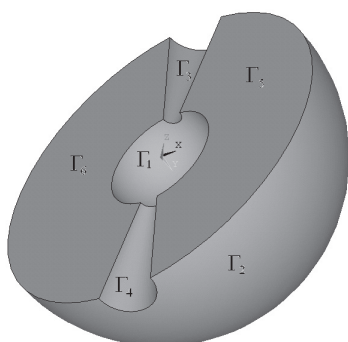


Fig. 4 A 3D image of one computational domain constructed using ANSYS

The radius of the spherical Earth in our experiment is $R = 6378$ km. Using the spherical coordinates (r, φ, λ) , where $r = |\vec{r}|$ is the radius, φ is the spherical geographical latitude and λ is the spherical geographical longitude, the two computational domains can be defined by the limits prescribed in Tab. 1. Both computational domains can be constructed using ANSYS by defining the 8 key points. The spherical and Cartesian coordinates of the key points are shown in Tab. 2.

Tab. 1 Limits of the computational domains in the spherical coordinates

	Computational domain	
	Eastern hemisphere	Western hemisphere
Interval for r (km)	(6378, 20000)	(6378, 20000)
Interval for φ (°)	(-80, 80)	(-80, 80)
Interval for λ (°)	(0, 180)	(-180, 0)

Inside the computational domain Ω , as the function T is harmonic (after proper treatment of the atmosphere), the Laplace differential equation must be valid.

$$\nabla^2 T = 0 \quad \text{in } \Omega. \quad (6)$$

The boundary of computational domain Ω consists of two concentric spherical surfaces (denoted as Γ_1 and Γ_2), two conical surfaces (Γ_3 and Γ_4) and two planar surfaces (Γ_5 and Γ_6), see Fig. 4. For our experiment we decided to combine the boundary conditions of the second kind (the Neumann type) on the two spherical surfaces, and the first kind (the Dirichlet type) on the two conical and two planar surfaces. Thus the boundary conditions can be written as follows

$$\frac{\partial T}{\partial n} = \delta g_{EGM2008} \quad \text{on } \Gamma_1 \quad (7)$$

$$\frac{\partial T}{\partial n} = -\delta g_{EGM2008} \quad \text{on } \Gamma_2 \quad (8)$$

$$T = T_{EGM2008} \quad \text{on } \Gamma_3 \cup \Gamma_4 \cup \Gamma_5 \cup \Gamma_6. \quad (9)$$

The boundary data was generated from the EGM2008 global geopotential model (Pavlis et al., 2008) using the GRAFIM software (Janák and Šprlák, 2006). For the spherical surfaces, the gravity disturbances were computed with a resolution of $1^\circ \times 1^\circ$ ($\Delta\varphi \times \Delta\lambda$), so that in one spherical surface, there are $161 \times 181 = 29141$ boundary values. For one computational domain, 58282 boundary values of gravity disturbances were computed. In a radial direction, each domain was divided into 60 layers of elements. On

Tab. 2 Coordinates of the 8 key points needed for the construction of the computational domain using ANSYS

Number of key point	Spherical coordinates			Cartesian coordinates		
	r (km)	φ (°)	λ (°)	X (km)	Y (km)	Z (km)
1	6378	80	0	1107.528	0.0	6281.104
2	6378	80	180	-1107.528	0.0	6281.104
3	6378	-80	0	1107.528	0.0	-6281.104
4	6378	-80	180	-1107.528	0.0	-6281.104
5	20000	80	0	3472.964	0.0	19696.155
6	20000	80	180	-3472.964	0.0	19696.155
7	20000	-80	0	3472.964	0.0	-19696.155
8	20000	-80	180	-3472.964	0.0	-19696.155

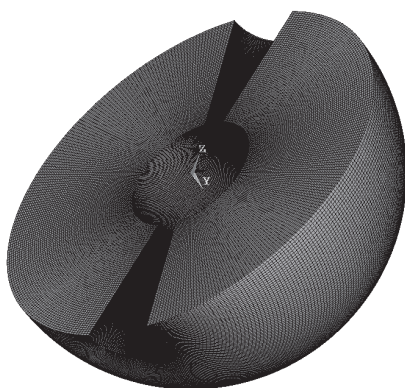


Fig. 5 A 3D computational domain after the meshing in ANSYS

the two conical parts of the boundary, the $61 \times 181 \times 2 = 22082$ boundary values of the disturbing potential (the Dirichlet type of boundary condition) were computed, and the $61 \times 161 \times 2 = 19642$ boundary values of the same type were computed on the two planar parts. Thus for one computational domain, a total of 100006 boundary values were computed. The boundary values on the planar parts of the boundary were common for both the Eastern and Western computational domains. The basic statistical parameters of the boundary values are presented in Tab. 3.

Before boundary values can be assigned to a particular part of a boundary in ANSYS, the meshing of the computational domain (the division of the domain into finite elements) first needs to be done. After the settings of the type of element and required resolution compatible with the resolution of the boundary values, the meshing in ANSYS is automatically

Tab. 3 Basic statistical parameters of the boundary values generated from EGM2008

Boundary	Number of values	Min.	Max.	Range	Mean	Standard deviation
Γ_1 East	29141	-293.59	280.34	573.92	0.395	37.807
Γ_1 West	29141	-266.31	281.98	548.29	-1.141	31.677
Γ_2 East	29141	-0.24	0.22	0.46	-0.005	0.097
Γ_2 West	29141	-0.14	0.16	0.30	-0.005	0.073
		(m ² ·s ⁻²)				
Γ_3 East	11041	0.54	359.80	359.26	16.71	34.25
Γ_3 West	11041	-20.27	375.09	395.35	20.83	44.29
Γ_4 East	11041	-510.32	94.41	604.74	-25.05	63.94
Γ_4 West	11041	-517.50	0.23	517.73	-37.71	72.73
Γ_5	9821	-48.32	524.52	572.85	55.24	74.87
Γ_6	9821	-606.44	504.73	1111.17	13.98	78.02

Tab. 4 Basic statistical parameters of the computed values of the disturbing potential in the merged computational domain

Number of values	Min.	Max.	Range	Mean	Standard deviation
	(m ² ·s ⁻²)				
3555200	-1029.6	803.3	1832.9	-2.9	76.4

performed. The type of element for our experiment was set as “Brick 8 node 70”. The computation domain after the meshing is shown in Fig. 5.

The total number of nodal points after the meshing is 1777600 for one computation domain.

The FEM method uses the so-called “weak formulation” of a boundary value problem and discretization to construct a system of linear equations. The matrix of this system of linear equations, usually called the stiffness matrix, is a sparse, symmetrical and positive definite. After solving this linear equation system, we get the unknown values of the disturbing potential T in all the nodal points of the computational domain. Here, we are skipping a detailed mathematical description of the solution, as it is not the purpose of this paper; it can be found elsewhere, see e.g. *Fašková (2008)* and *Fašková et al. (2010)*.

After computation of the boundary value problem in both computational domains, i.e. the Eastern and Western domains, the results were merged into one file. The basic statistics of the computed values of T are shown in Tab. 4.

As an example of the visualization of our results, we present a sequence of the pictures of the equipotential surface of the disturbing potential $T(\vec{r})=0$ produced by Voxler® (Volumetric Visualization Package), see Appendix 1. Based on this visualization and an analysis of the numerical results, we can get an idea about the behavior of the disturbing potential in the space around the Earth and comment on some properties of the equipotential surfaces of the disturbing potential $T(\vec{r})=const$. The most important properties are summarized in the conclusion.

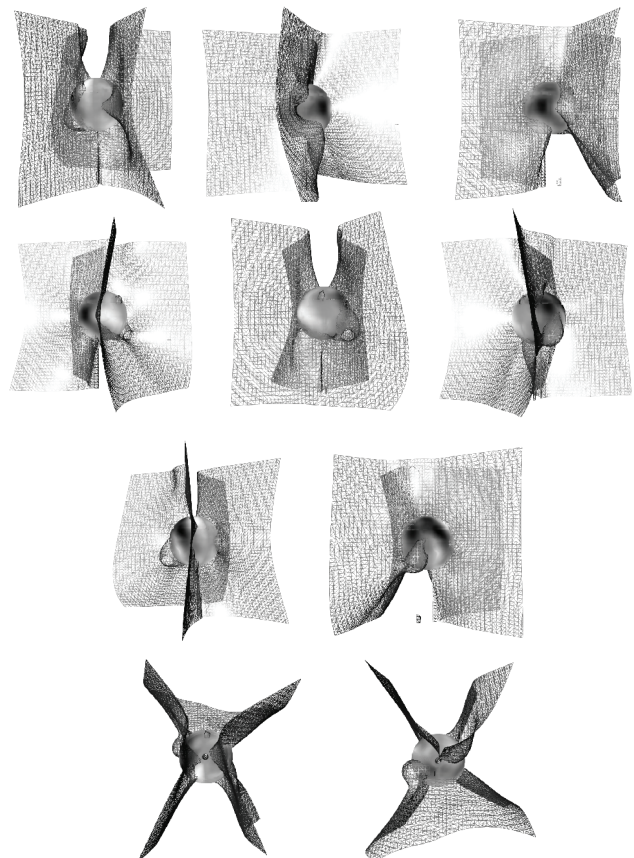
Let us also mention one theoretical aspect of our solution. The computational domain where the disturbing potential satisfies the Laplace differential equation is originally infinite, and the property of regularity in infinity must be fulfilled. For the FEM solution we have to restrict the upper boundary of the computational domain at a certain finite altitude; thus, we cannot use the regularity condition directly in our solution. However, the calibrated and validated satellite measurements in the upper restricted boundary, e.g. the GOCE measurements in the near future, should adequately replace the regularity condition.

4 CONCLUSION

Based on Tab. 4 we can see that the mean value of the disturbing potential in the computational domain is negative. Appendix 1 also documents that the larger volume around the Earth possesses negative values of the disturbing potential. The positive values of the disturbing potential are mostly concentrated around the meridians 0° and 180°.

In summarising the results we can make the following statements:

- The equipotential surface $T(\vec{r})=0$ is mostly vertical and open to infinity; it resembles a funnel, see Appendix 1;
- In the vicinity of the equipotential surface $T(\vec{r})=0$, the gravity disturbance vector is almost horizontal (the horizontal component



A sequence of plots of the equipotential surface $T(\vec{r})=0$ above the solution on the Earth's surface. The Z-axis on the first 8 plots points up. The facing meridian starts from 0° (top left) with a step of 45°. The last 2 plots are polar views: the north pole (left), and the south pole (right).

dominates), and the vertical component dominates in the vicinity of the local maxima and minima;

- Other equipotential surfaces of the disturbing potential above the Earth's surface are closed relative to the Earth's surface and resemble a balloons or piles;
- It is very difficult at a high altitude to estimate the exact location of an equipotential surface $T(\vec{r}) = 0$, because the gradient of T becomes very small.

One very valuable advantage of the solution presented is the possibility of combining satellite and terrestrial data into one solution in a natural way, i.e. by combining the different sources to

generate the boundary values. The spatial model of the disturbing potential around the Earth based on actual satellite and terrestrial data will hopefully be computed in the near future. Such a model can serve a variety of applications, e.g. an investigation of a deep Earth mass anomaly structure or the design of optimal low Earth orbits for various satellites.

Acknowledgements

The research presented in this paper was supported by Slovak national projects VEGA 1/0775/08, APVV-0351-07 and VEGA 1/0269/09.

REFERENCES

- **Brenner, S. C. - Scott, L. R. (2002)** The Mathematical Theory of Finite Element Methods. 2nd ed. Springer – Verlag, New York.
- **Fašková, Z. (2008)** Numerical methods for solving a geodetic boundary value problem. PhD. thesis. Slovak University of Technology, Bratislava.
- **Fašková, Z. - Čunderlík R. - Mikula, K. (2010)** Finite Element Method for solving geodetic boundary value problems. Journal of Geodesy, 84, 2, pp. 135-144.
- **Hofmann-Wellenhof, B. - Moritz, H. (2005)** Physical Geodesy. Springer, Vienna, New York.
- **Janák, J. - Šprlák, M. (2006)** Nový počítačový program na modelovanie tiažového poľa pomocou sférických harmonických funkcií. (A new software for gravity field modelling using spherical harmonics). Geodetický a kartografický obzor, 52/94, 1/06, pp. 1-8.
- **Pavlis, N. K. - Holmes, S. A. - Kenyon, S. C. - Factor, J. K. (2008)** An earth gravitational model to degree 2160 EGM2008. Geophysical Research Abstracts EGU 2008.
- **Vaniček, P. - Krakiwsky, E. J. (1986)** Geodesy – the Concepts. Elsevier, Amsterdam.